

# Proton Transport by Phosphate Diffusion — A Mechanism of Facilitated CO<sub>2</sub> Transfer

GEROLF GROS, WALDEMAR MOLL, HEIKE HOPPE, and HANNE GROS

From the Institut für Physiologie, Universität Regensburg, 8400 Regensburg, West Germany

**ABSTRACT** We have measured CO<sub>2</sub> fluxes across phosphate solutions at different carbonic anhydrase concentrations, bicarbonate concentration gradients, phosphate concentrations, and mobilities. Temperature was 22–25°C, the pH of the phosphate solutions was 7.0–7.3. We found that under physiological conditions of pH and pCO<sub>2</sub> a facilitated diffusion of CO<sub>2</sub> occurs in addition to free diffusion when (a) sufficient carbonic anhydrase is present, and (b) a concentration gradient of HCO<sub>3</sub><sup>-</sup> is established along with a pCO<sub>2</sub> gradient, and (c) the phosphate buffer has a mobility comparable to that of bicarbonate. When the phosphate was immobilized by attaching 0.25-mm-long cellulose particles, no facilitation of CO<sub>2</sub> diffusion was detectable. A mechanism of facilitated CO<sub>2</sub> diffusion in phosphate solutions analogous to that in albumin solutions was proposed on the basis of these findings: bicarbonate diffusion together with a facilitated proton transport by phosphate diffusion. A mathematical model of this mechanism was formulated. The CO<sub>2</sub> fluxes predicted by the model agree quantitatively with the experimentally determined fluxes. It is concluded that a highly effective proton transport mechanism acts in solutions of mobile phosphate buffers. By this mechanism, CO<sub>2</sub> transfer may be increased up to fivefold and proton transfer may be increased to 10,000-fold.

## INTRODUCTION

The pH value of the interior of living cells is held constant within narrow limits. In the cells of mammals including man a pH value of about 7 is maintained in spite of a continuous production of CO<sub>2</sub> and fixed acids (e.g. lactic acid) inside the cells. This holds true also for those cells of the gastric mucosa and the kidney which are specialized in secreting large amounts of H<sup>+</sup> (2). Thus, H<sup>+</sup> and CO<sub>2</sub> have to be constantly and efficiently transported through the cell interior before they permeate the cell membrane. This paper is aimed at elucidating possible mechanisms of intracellular proton and CO<sub>2</sub> transfer.

Production as well as secretion of H<sup>+</sup> establish gradients of pH within the cell along which proton fluxes matching the rates of secretion or production have to occur. Free diffusion of protons appears to be a rather ineffective mechanism of proton transport since at physiological values of pH its driving force is extremely small: H<sup>+</sup> concentration differences in cells are of the order of 10<sup>-7</sup>–10<sup>-8</sup> M. However, due to the buffering substances of the cell, such a H<sup>+</sup> concentration difference is accompanied by a concentration difference of buffered protons of the order of 10<sup>-2</sup>–10<sup>-3</sup> M. Although the mobility of the buffers may be 10–100

times lower than the mobility of free protons, a facilitated transport of protons by buffer diffusion should thus be 1,000–10,000 times more effective than free diffusion of protons (1, 3, 4). An analogous consideration led to the conclusion that oxyhemoglobin diffusion can produce a significant facilitation of oxygen diffusion (5–10). However, facilitated O<sub>2</sub> diffusion under physiological conditions appears to be a mechanism far less effective than facilitated H<sup>+</sup> diffusion since the O<sub>2</sub> fluxes provided by it are only of the same order as those provided by free diffusion of oxygen (7, 9–11).

Proton transport together with diffusion of fixed acid anions (such as lactate) result in fixed acid transfer, proton transport together with bicarbonate diffusion result in carbonic acid transfer, and, with the action of CO<sub>2</sub> hydration-dehydration reaction, CO<sub>2</sub> transfer. Measurements of CO<sub>2</sub> net fluxes across buffer solutions should therefore allow quantitative inferences on the transfer of protons in such a system. In the present study we report determinations of CO<sub>2</sub> fluxes across layers of phosphate buffer solutions under various conditions of CO<sub>2</sub> hydration velocity, pCO<sub>2</sub>, buffer concentration, and buffer mobility. The results and calculations indicate that (a) buffer diffusion indeed enhances proton transport by several orders of magnitude, and (b) this mechanism of proton transport together with bicarbonate diffusion make possible, in the presence of carbonic anhydrase, a facilitation of CO<sub>2</sub> diffusion, which under physiological conditions of pH and pCO<sub>2</sub> can increase the flux of CO<sub>2</sub> to 2.5–5-fold.

As a buffer we have chosen phosphate for the present experiments, since it is an important buffer in many tissues (muscle, kidney, digestive tract) and because facilitated CO<sub>2</sub> transfer in phosphate solutions, unlike that in protein solutions (1, 3), allows a straightforward physicochemical analysis. Taking into account the diffusion coefficients of the various molecular species involved as well as the magnitude of the diffusion potential, a complete theoretical treatment of facilitated CO<sub>2</sub> diffusion in buffer solutions was possible for the first time. In addition, the availability of cellulose phosphate P11, whose phosphate groups are potent buffers but practically immobilized through attachment to cellulose particles as large as 30–250 μm, allows a direct demonstration of the crucial role of buffer mobility for the facilitated diffusion of CO<sub>2</sub>.

## METHODS

### *Principle*

CO<sub>2</sub> fluxes across 180-μm or 2-mm-thick layers of the solutions to be investigated were measured under steady-state conditions. The details of the method have been described elsewhere (12). In brief, the layers were put between two chambers which were perfused with CO<sub>2</sub>-N<sub>2</sub> mixtures of different CO<sub>2</sub> partial pressures. When steady state was reached, the CO<sub>2</sub> concentrations prevailing in the two chambers were measured. The CO<sub>2</sub> concentrations allowed to calculate the CO<sub>2</sub> partial pressure difference across the layer, and, together with the flow rates of the gases, the flux of CO<sub>2</sub> resulting from this CO<sub>2</sub> partial pressure difference.

### *Layers*

Millipore filters with an effective thickness of 180 μm (type HA, Millipore Corp., Bedford, Mass.) were used for the experiments with solutions of inorganic phosphate. The filters were soaked in these solutions for 30 min. Since the flow rates of the gases

passing through the chambers were generally lower than in previous studies (1, 3, 12), the filters did not have to be covered by silicone membranes to prevent exsiccation. Two-millimeter-thick, filter-free layers were used for the experiments with cellulose phosphate P11. It was not possible to employ Millipore filters in these experiments because the cellulose phosphate particles are considerably larger than the pores of the filters (0.45  $\mu\text{m}$ ). Instead, the solutions were filled in between two 150- $\mu\text{m}$ -thick silicone membranes stretched out at a distance of 2 mm. In calculating the  $\text{CO}_2$  diffusion coefficients the diffusion resistance of these membranes (5–20% of the total diffusion resistance of the layers) was taken into account.

### *Materials*

Solutions of inorganic phosphate were prepared by dissolving mixtures of  $\text{Na}_2\text{HPO}_4$  and  $\text{KH}_2\text{PO}_4$  (p.a., Merck Company, Darmstadt) in distilled water. Suspensions of cellulose phosphate were obtained by suspending cellulose phosphate P11 (Whatman Ltd., Springfield Mill, Maidstone, Kent) in a 50 mM NaCl solution. The "fines" were carefully removed from the P11 suspensions by the following procedure: A suspension of 140 g of dry cellulose phosphate in 31 of 50 mM NaCl was allowed to settle in a 80-cm-high cylinder for 15 min. Then the supernatant containing the smaller particles of cellulose phosphate was removed, and the pellet containing the larger particles was resuspended in the same volume of NaCl solution. After repeating this procedure 20 times 22 g of cellulose phosphate representing the fraction of larger particles were recovered from the original 140 g. These selected cellulose phosphate particles had a rod-like shape with an average length of 250  $\mu\text{m}$  (SD  $\pm$  70  $\mu\text{m}$ ) and an average diameter of 31  $\mu\text{m}$  (SD  $\pm$  5  $\mu\text{m}$ ) as determined microscopically. Solutions of 8 g/100 ml cellulose phosphate in 1.5 g/100 ml agar-agar were prepared using cellulose phosphate rendered free of smaller particles as described above. A 16-g/100 ml solution of cellulose phosphate whose pH had been adjusted to 7.43 was warmed up to 45°C and mixed with an equal volume of 3-g/100 ml fluid agar-agar solution of the same temperature. From this mixture, while still at 45°C, 2-mm-thick diffusion layers were prepared. The mixture gelatinized when the layers were cooled to room temperature. The agar-agar gel prevented sedimentation of the cellulose phosphate particles during the diffusion experiment. Solutions of 90 mM phosphate in 1.5-g/100 ml agar-agar were obtained in the same fashion. The 16-g/100 ml cellulose phosphate solution was replaced by a 180 mM solution of inorganic phosphate with pH = 7.43. The carbonic anhydrase added in part of the experiments was bovine carbonic anhydrase purchased from Serva (Heidelberg). Its activity was 11 at a concentration of 1 mg/liter according to the suppliers.

### *Analytical Procedures*

$\text{CO}_2$  concentrations of the gases were measured in a gaschromatograph (carrier gas: helium 40 ml/min, column: Porapak, OD  $\frac{1}{4}$  inch, length 126 cm). Cellulose phosphate concentrations were obtained from dry weight determinations. Titration curves were done using Radiometer (Copenhagen) automatic titration equipment with a thermostatted titration vessel. The  $\text{CO}_2$  binding of phosphate solutions was studied in solutions of 49 mM  $\text{Na}_2\text{HPO}_4$  with 17 mM  $\text{KH}_2\text{PO}_4$  and 666 mM  $\text{Na}_2\text{HPO}_4$  with 39 mM  $\text{KH}_2\text{PO}_4$ . The solutions were equilibrated at 25°C with  $\text{CO}_2$ - $\text{N}_2$  mixtures of known  $p\text{CO}_2$  in Laue-tonometers (13). Subsequently the total content of  $\text{CO}_2$  was determined in a Van Slyke manometric apparatus, and the pH value was measured anaerobically in a thermostatted capillary pH glass electrode.

## RESULTS AND DISCUSSION

The results described in the following sections demonstrate facilitated  $\text{CO}_2$  diffusion in phosphate solutions and show that under the present experimental

conditions there are three prerequisites for facilitation: (A) the catalyzing action of carbonic anhydrase, (B) the formation of a concentration gradient of bicarbonate across the layer, and (C) the presence of mobile buffers acting as proton carriers.

#### (A) Carbonic Anhydrase

When carbonic anhydrase is added to solutions of inorganic phosphate the flux of  $\text{CO}_2$  increases severalfold: facilitated diffusion of  $\text{CO}_2$  occurs. This is demonstrated in Fig. 1 where the  $\text{CO}_2$  flux across 180- $\mu\text{m}$ -thick layers of phosphate solutions at constant  $\text{CO}_2$  boundary partial pressures is plotted as a function of the carbonic anhydrase concentration. All experiments were performed at room temperature (22–25°C).

Fig. 1a shows that in the absence of carbonic anhydrase the  $\text{CO}_2$  flux across the 66 mM phosphate solution amounted to  $1.3 \text{ nmol cm}^{-2}\text{s}^{-1}$ . With  $\text{CO}_2$  partial pressures at the boundaries of the layers of 57 and 26 torr this corresponds to a  $\text{CO}_2$  diffusion coefficient of  $D_{\text{CO}_2} = 15.9 \cdot 10^{-6} \text{ cm}^2\text{s}^{-1}$  (see Table I). This value is 3% lower than the value obtained under identical conditions for pure water ( $D_{\text{CO}_2} = 16.4 \cdot 10^{-6} \text{ cm}^2\text{s}^{-1}$ ). Such a reduction would be expected from the data of Ratcliff and Holdcroft (16) on the effects of various salts on the diffusivity of  $\text{CO}_2$ . The good agreement of the two diffusion coefficients thus indicates that (in spite of the slight catalytic effect of phosphate on the hydration of  $\text{CO}_2$  [17]) in phosphate solution without carbonic anhydrase, as in water (1), no facilitation of  $\text{CO}_2$  diffusion occurs. Facilitation is observed, however, when carbonic anhydrase is added. A maximum  $\text{CO}_2$  flux of  $3.2 \text{ nmol cm}^{-2}\text{s}^{-1}$  is reached with a carbonic anhydrase concentration of 0.2 g/100 ml. This flux seems to be unlimited by the velocity of  $\text{CO}_2$  hydration since further increase of the carbonic anhydrase concentration does not lead to a further increase of the  $\text{CO}_2$  flux. With sufficient carbonic anhydrase present, facilitated diffusion can thus increase the  $\text{CO}_2$  transfer 2.5 times in a 66 mM phosphate solution under fairly physiological conditions (boundary  $\text{pCO}_2$ 's 57 and 26 torr, average pH  $\sim 7.0$ ).

Fig. 1b shows  $\text{CO}_2$  fluxes through a 705 mM phosphate solution plotted versus carbonic anhydrase concentration. In the absence of carbonic anhydrase a flux of  $0.69 \text{ nmol cm}^{-2}\text{s}^{-1}$  was measured when the boundary  $\text{CO}_2$  partial pressures were 56 and 30 torr, respectively. Due to the high concentration of salts the corresponding value of the  $\text{CO}_2$  diffusion coefficient (Table I) is reduced by 22% as compared to that in water. Again, the flux of  $\text{CO}_2$  increases with carbonic anhydrase concentration: it reaches a maximum of  $3.4 \text{ nmol cm}^{-2}\text{s}^{-1}$  with carbonic anhydrase concentrations  $\geq 0.2 \text{ g/100 ml}$ . Thus, facilitated diffusion in this case causes a five-fold increase in  $\text{CO}_2$  transfer. It may be noteworthy that a more than 10-fold increase of the phosphate concentration leads to an increase of only 1.7-fold of the maximal  $\text{CO}_2$  fluxes per  $\text{CO}_2$  partial pressure difference and of the maximal  $\text{CO}_2$  diffusion coefficients (see Table I).

#### (B) Concentration Gradient of $\text{HCO}_3^-$

Since facilitated diffusion of  $\text{CO}_2$ , as shown above, requires considerable acceleration of the  $\text{CO}_2$  hydration reaction by carbonic anhydrase, the conclusion that it

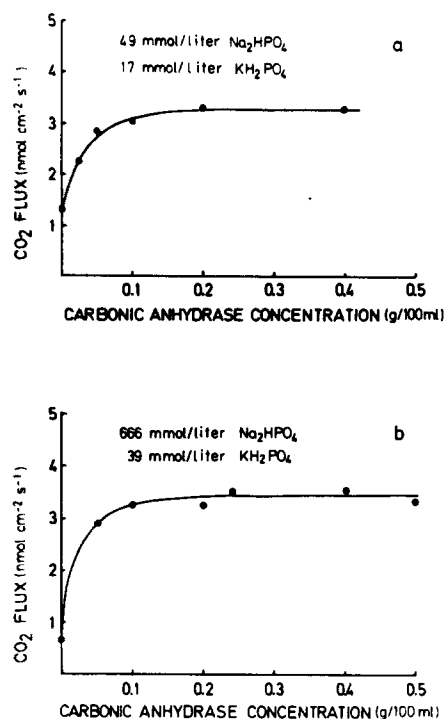


FIGURE 1. Flux of CO<sub>2</sub> across 180- $\mu$ m-thick layers of 66 mM (Fig. 1 a) and 705 mM (Fig. 1 b) phosphate solution as a function of carbonic anhydrase concentration. The layers were Millipore filters with an effective diffusion area of 8.56 cm<sup>2</sup>. Temperature: 22–25°C. The CO<sub>2</sub> boundary partial pressures were held constant (for the 67 mM solution at 57/26 torr, for the 705 mM solution at 56/30 torr) in spite of CO<sub>2</sub> fluxes changing with the carbonic anhydrase concentration by varying the rate of gas flowing through the chambers.

TABLE I  
CO<sub>2</sub> DIFFUSION COEFFICIENTS IN 66 AND 705 mM PHOSPHATE SOLUTIONS

Phosphate concentration	CO <sub>2</sub> diffusion coefficients	Carbonic anhydrase concentration	Boundary CO <sub>2</sub> partial pressures	Average pH in the layer
mM	cm <sup>2</sup> s <sup>-1</sup>	g/100 ml	torr	
0	16.4 · 10 <sup>-6</sup> (±0.9%)	—		
66	15.9 · 10 <sup>-6</sup> (±1.9%)	—	57/26	7.0
66	39.2 · 10 <sup>-6</sup> (±2.9%)	≥ 0.2	57/26	7.0
705	13.4 · 10 <sup>-6</sup> (±2.4%)	—	56/30	7.3
705	67.3 · 10 <sup>-6</sup> (±2.3%)	≥ 0.2	56/30	7.3

CO<sub>2</sub> diffusion coefficients (with standard error as percentage of the mean) in 66 and 705 mM phosphate solutions, in presence of excess and in absence of carbonic anhydrase. Layers: Millipore filters with an effective thickness of 180  $\mu$ m. Temperature: 22–25°C. The diffusion coefficients are calculated from the data of Fig. 1 using the following CO<sub>2</sub> solubility coefficients: 49 nmol cm<sup>-3</sup> torr<sup>-1</sup> in water (14), 48 and 35 nmol cm<sup>-3</sup> torr<sup>-1</sup> in the 66 and 705 mM phosphate solution, respectively (15). The average pH values are calculated from the average pCO<sub>2</sub>'s and the buffer capacities.

involves diffusion of the product of this reaction, bicarbonate, seems obvious. The same suggestion has, indeed, been made by several authors, who studied facilitated  $\text{CO}_2$  net fluxes in protein solutions (1, 3, 18) and in highly alkaline carbonate-bicarbonate solutions (19, 20), or bicarbonate self-exchange under conditions of zero net fluxes (21, 22). If it is true for our system, we should expect facilitated  $\text{CO}_2$  diffusion to depend, among other parameters, on the concentration gradient of bicarbonate. Fig. 2 demonstrates that this is the case: it shows a plot of the facilitated flux of  $\text{CO}_2$  versus the concentration difference of bicarbonate across the layer. Different bicarbonate concentration gradients were established by varying the  $\text{CO}_2$  boundary partial pressures. All experiments were carried out in the presence of an excess of carbonic anhydrase ( $>0.2$  g/100 ml). Fig. 2 shows that, for the 66 mM as well as for the 705 mM phosphate solution, the facilitated flux of  $\text{CO}_2$  is proportional to the bicarbonate concentration difference across the layer. It will be noted that the facilitated flux per  $\text{HCO}_3^-$  concentration difference in the 705 mM solution is only half of that in the 66 mM solution which results mainly from the decreased activity of the bicarbonate ion in the more concentrated solution (see Table III). We may conclude that the data of Fig. 2 confirm the view that bicarbonate diffusion is an essential element of facilitated  $\text{CO}_2$  diffusion.

#### (C) Buffer Mobility

If bicarbonate diffuses across the layer after a concentration gradient to enhance the transport of  $\text{CO}_2$ , it will be formed by the catalyzed  $\text{CO}_2$  hydration reaction at the side exposed to a high  $p\text{CO}_2$ , and decomposed to form  $\text{CO}_2$  at the side exposed to a low  $p\text{CO}_2$  (see Fig. 4). Formation of  $\text{HCO}_3^-$  from  $\text{CO}_2$  then leads to a release of  $\text{H}^+$  at the side of high  $p\text{CO}_2$ , the reverse reaction leads to a consumption of  $\text{H}^+$  at the side of low  $p\text{CO}_2$ . Therefore, as has been pointed out before (1, 3, 23), facilitated  $\text{CO}_2$  transport by bicarbonate diffusion under steady-state conditions requires equivalent fluxes of bicarbonate and protons. It has been mentioned in the introduction that free diffusion of protons cannot provide these fluxes: judging from the boundary pH values of the layers (6.89 and 7.07, see below) and the  $\text{H}^+$  diffusion coefficient ( $92 \cdot 10^{-6} \text{ cm}^2\text{s}^{-1}$  [24]), free diffusion can account for a proton flux of about 1/10,000 of the measured facilitated  $\text{CO}_2$  flux. The mechanism which is able to produce proton fluxes 10,000 times as large as those by free diffusion, is a facilitated proton transfer by phosphate diffusion as will be shown by the calculations described in the next section. If this process, together with the diffusion of bicarbonate, are indeed the basis of facilitated  $\text{CO}_2$  diffusion, facilitated diffusion should be abolished when the buffer is immobilized. In the experiments described in this section the diffusion of  $\text{CO}_2$  through solutions of mobile phosphate buffer was compared with that through solutions of immobile phosphate buffer.

In the first two lines of Table II, the  $\text{CO}_2$  diffusion coefficients measured in 8-g/100 ml cellulose phosphate solution with 1.5 g/100 ml gelatinized agar-agar and excess carbonic anhydrase are listed. This solution does not contain freely diffusible buffers. The phosphate groups are covalently bound to rod-shaped cellulose particles with an average diameter of 31  $\mu\text{m}$  and an average length of

250  $\mu\text{m}$ . Using Einstein's (25) relation between molecular radius and diffusion coefficient it can be estimated that the diffusion of these cellulose particles is 50,000–1,000,000 times slower than the diffusion of free phosphate ions. In addition the presence of gelatinized agar-agar will inhibit the diffusion of the cellulose phosphate particles (as it inhibits their sedimentation). Whereas the mobility of the phosphate thus should be practically abolished in the cellulose phosphate solution, its capability of acting as a buffer is preserved. This is demonstrated in Fig. 3 which shows the titration curve of a 16 g/100 ml cellulose phosphate solution. From this solution, which has a buffer capacity of  $\sim 90 \text{ mM}/\Delta\text{pH}$ , 2-mm-thick filter-free layers were prepared after mixing with equal volumes of 3-g/100 ml agar-agar.  $\text{CO}_2$  diffusion coefficients were determined in these layers in a low and in a high  $\text{CO}_2$  partial pressure range at 22–25°C. The

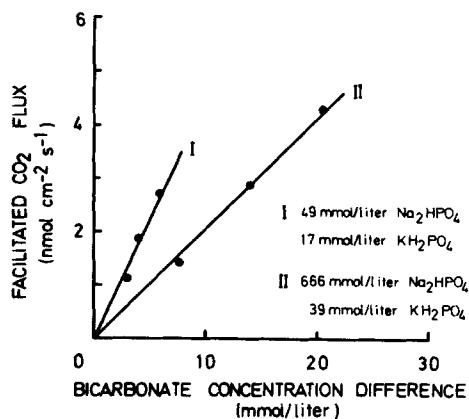


FIGURE 2

FIGURE 2. Facilitated flux of  $\text{CO}_2$  as a function of the bicarbonate concentration difference across the layer, for 66 mM (I) and 705 mM (II) phosphate solution. Layers: Millipore filters, effective thickness 180  $\mu\text{m}$ . Carbonic anhydrase concentration  $\geq 0.2 \text{ g}/100 \text{ ml}$ . Temperature: 22–25°C. The boundary concentrations of bicarbonate were varied by exposure of the layers to different boundary  $\text{CO}_2$  partial pressures and were read from the  $\text{CO}_2$  binding curve of the pertinent solution (they were practically identical to those obtained from the more exact calculations described below). The facilitated flux was obtained as (measured total flux) – (concentration gradient of dissolved  $\text{CO}_2$ )  $\times$  ( $\text{CO}_2$  diffusion coefficient representing free diffusion only). The facilitated flux per bicarbonate concentration gradient is  $8.0 \cdot 10^{-6} \text{ cm}^2\text{s}^{-1}$  for the 66 mM, it is  $3.7 \cdot 10^{-6} \text{ cm}^2\text{s}^{-1}$  for the 705 mM phosphate solution. Both figures are close to the respective diffusion coefficients of bicarbonate (see Table III).

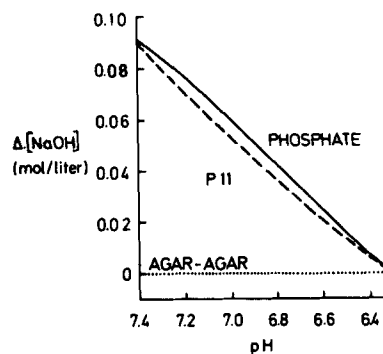


FIGURE 3

FIGURE 3. Titration curves of the solutions used for the diffusion experiments of Table II: 180 mM inorganic phosphate, 16 g/100 ml cellulose phosphate P11 (in 50 mM NaCl), and 3 g/100 ml agar-agar. The temperature is 25°C for the phosphate and the P11 solution, and 45°C for the agar-agar. The buffer capacity between pH 6.6 and pH 7.2 is about the same for the phosphate and the P11 solution ( $\sim 90 \text{ mM}/\Delta\text{pH}$ ). Agar-agar shows no detectable buffer capacity and thus cannot contribute significantly to proton binding and proton transport in the diffusion experiments.

results show that no facilitated diffusion of  $\text{CO}_2$  occurs in cellulose phosphate solutions: (a) The  $\text{CO}_2$  diffusion coefficients obtained in the two partial pressure ranges ( $\text{CO}_2$  boundary partial pressures 71/8 torr, and 685/69 torr, respectively) are not significantly different. Thus, they behave like diffusion coefficients describing free diffusion of  $\text{CO}_2$  only. A facilitation of  $\text{CO}_2$  diffusion, and with it the  $\text{CO}_2$  diffusion coefficient, should increase when the  $\text{CO}_2$  partial pressure range is lowered (see Fig. 6). (b) The values of the  $\text{CO}_2$  diffusion coefficients in both partial pressure ranges are about 25% lower than the value in water (Table I). Such a reduction is to be expected for free diffusion of  $\text{CO}_2$  if it is attributed to the diminution of the water space by the cellulose particles: taking into account the different densities of protein and cellulose phosphate, this reduction agrees well with the relation between the  $\text{CO}_2$  diffusion constant and protein concentration described by Gros and Moll (12). Again, there is no indication for a facilitated  $\text{CO}_2$  diffusion in cellulose phosphate solutions.

Lines 3 and 4 of Table II show the results of diffusion experiments with 90 mM solution of inorganic phosphate. Again, 1.5 g/100 ml gelatinized agar-agar and excess carbonic anhydrase were present. Fig. 3 and Table II show that the following parameters were practically identical in this solution and in the 8-g/100 ml cellulose phosphate solution: buffer capacity,  $\text{CO}_2$  partial pressure ranges, average pH values in the layers, carbonic anhydrase concentration, agar-agar concentration, and layer thickness. However, contrary to the cellulose phosphate solution, the phosphate ions are free to diffuse in this case (1.5-g/100 ml agar-agar has only a small inhibitory effect of a few percent on the diffusion of gases and small ions [1, 26, 27]). Table II shows that mobility of the phosphate results in a facilitation of  $\text{CO}_2$  diffusion: (a) The  $\text{CO}_2$  diffusion coefficient obtained in the low partial pressure range (66/21 torr) is 2.1 times higher than that determined in the high partial pressure range (676/118 torr). A similar dependency of the  $\text{CO}_2$  diffusion coefficient on the  $\text{CO}_2$  partial pressure range has previously been observed for the diffusion of  $\text{CO}_2$  through hemoglobin and albumin solutions (1, 3, 23). (b) The  $\text{CO}_2$  diffusion coefficients in both partial pressure ranges are higher than the value determined for water ( $16.4 \cdot 10^{-6} \text{ cm}^2 \text{ s}^{-1}$ , see Table I). This suggests that facilitated diffusion not only occurs in the low but also in the high partial pressure range. As estimated from the value of  $D_{\text{CO}_2}$  in the 66 mM phosphate solution without carbonic anhydrase (Table I), facilitated diffusion causes a 1.5-fold increase in  $\text{CO}_2$  flux in the high, and a 3.1-fold increase in the low partial pressure range. We conclude from the results of Table II that the mere presence of buffers is not sufficient for facilitated  $\text{CO}_2$  diffusion to occur; the mobility of the buffers is a necessary condition.

#### THEORY

The model of facilitated  $\text{CO}_2$  diffusion in phosphate solutions developed on the basis of the described experimental results (A-C) is depicted in Fig. 4: At the side of the diffusion layer which is exposed to a high  $\text{CO}_2$  partial pressure,  $\text{CO}_2$  is hydrated with the catalyzing action of carbonic anhydrase (A). This reaction produces equal amounts of bicarbonate and protons. The bicarbonate diffuses across the layer after a concentration gradient (B). The protons are, practically

TABLE II  
CO<sub>2</sub> DIFFUSION COEFFICIENTS IN SOLUTIONS OF CELLULOSE  
PHOSPHATE P11 AND OF INORGANIC PHOSPHATE

Material	CO <sub>2</sub> diffusion coefficient	Boundary CO <sub>2</sub> partial pressures	Average pH in the layer	Carbonic anhydrase concentration
		<i>torr</i>		<i>g/100 ml</i>
8 g/100 ml cellulose phosphate P11, in 1.5 g/100 ml agar-agar	13.1 · 10 <sup>-6</sup> (±4.5%) 12.2 · 10 <sup>-6</sup> (±7.7%)	71/8 685/69	7.2 6.7	0.2 0.2
90 mM inorganic phosphate, in 1.5 g/100 ml agar-agar	48.6 · 10 <sup>-6</sup> (±1.1%) 23.0 · 10 <sup>-6</sup> (±1.4%)	66/21 676/118	7.1 6.6	0.2 0.2

CO<sub>2</sub> diffusion coefficients (with standard error as percentage of the mean) in 8 g/100 ml cellulose phosphate P11 and 90 mM inorganic phosphate solutions. The diffusion measurements were performed in a low and a high CO<sub>2</sub> partial pressure range using 2-mm-thick filter-free layers. The CO<sub>2</sub> solubility coefficient used to calculate CO<sub>2</sub> diffusion coefficients from the measured CO<sub>2</sub> fluxes is 47 nmol cm<sup>-3</sup> torr<sup>-1</sup> for both solutions (for 90 mM phosphate estimated from reference 15, for cellulose phosphate from its concentration and specific volume, 0.5 ml g<sup>-1</sup>). The average pH values are calculated from the average pCO<sub>2</sub>'s in the layers and the buffer capacities of the solutions (see Fig. 3).

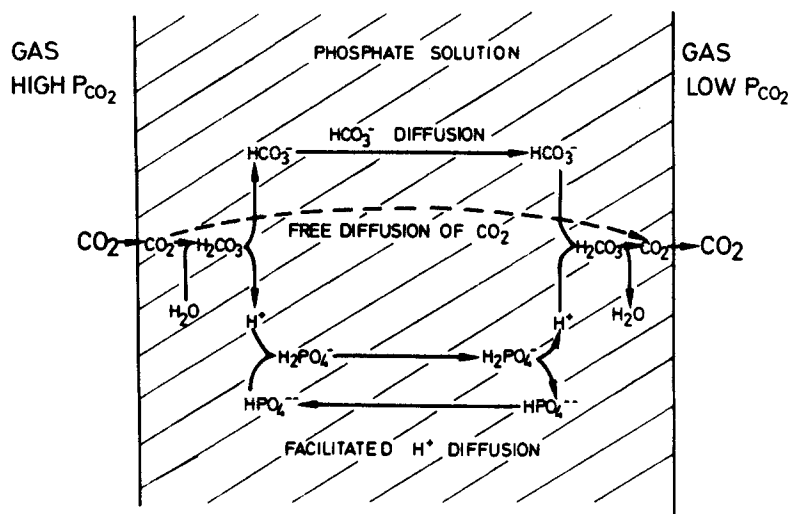


FIGURE 4. Model of CO<sub>2</sub> diffusion in phosphate solutions: Besides free diffusion of CO<sub>2</sub>, a facilitated diffusion of CO<sub>2</sub> occurs which is based on diffusion of bicarbonate and facilitated proton transport by phosphate diffusion.

completely and instantaneously, taken up by divalent phosphate ions. These act as proton carriers in this system (C): monovalent phosphate diffuses across the layer together with bicarbonate. At the side of low pCO<sub>2</sub> (and high pH) protons dissociate from H<sub>2</sub>PO<sub>4</sub><sup>-</sup>, and recombine with HCO<sub>3</sub><sup>-</sup> to form, again catalyzed by carbonic anhydrase (A), CO<sub>2</sub> which leaves the layer. HPO<sub>4</sub><sup>--</sup>, the unloaded

proton carrier, diffuses back (C) to the side of high  $p\text{CO}_2$  to take up new protons. Aside from the experimental evidence presented here this scheme is in agreement with the finding of Meldon et al. (28) that facilitated diffusion of  $\text{CO}_2$ , at a given pH, reaches a maximum when the pK of a buffer present in the solution roughly agrees with the pH, i.e. when the buffer capacity of the solution is close to its maximum. Evidence for an analogous mechanism of facilitated  $\text{CO}_2$  diffusion in protein solutions has been given by Gros and Moll (1, 3, 23). Buffer-facilitated proton transport has also been considered by Engasser and Horvath (4) in theoretical studies on the pH profile of bound enzymes.

It may be of interest to compare the mechanism of facilitated oxygen diffusion in hemoglobin solutions with the model proposed here for facilitated  $\text{CO}_2$  diffusion in phosphate solutions. In the former case a flux of  $\text{O}_2$  bound to hemoglobin is linked to a flux of dissolved  $\text{O}_2$ . Both fluxes can simply be expressed by Fickian diffusion equations, one for the free and one for the bound species (5, 6, 8-10). In the case of facilitated  $\text{CO}_2$  diffusion (a) a flux of bicarbonate, and (b) a flux of buffered protons (the latter representing a facilitated diffusion process in itself) occur simultaneously with a flux of dissolved  $\text{CO}_2$ . The fluxes of the ions involved cannot be described in terms of simple diffusion processes since electrical potentials play an important role as the calculations described in the following paragraphs will show.

#### *Basic Equations and Numerical Solutions*

The flux,  $F_i$ , of each substance present in the layer can be expressed by the Nernst-Planck equation:

$$F_i = -D_i \cdot \frac{dC_i}{dx} - D_i \cdot \frac{z_i F}{RT} \cdot C_i \cdot \frac{d\phi}{dx}, \quad (1)$$

where the index  $i$  refers to the following species involved:  $\text{HCO}_3^-$ ,  $\text{H}_2\text{PO}_4^-$ ,  $\text{HPO}_4^{--}$ ,  $\text{Na}^+$ ,  $\text{K}^+$ , and  $\text{CO}_2$ .  $D_i$  is the diffusion coefficient of species  $i$ ,  $C_i$  its concentration,  $z_i$  its charge,  $\phi$  is the electrical potential,  $F$  the Faraday constant,  $R$  the gas constant, and  $T$  the absolute temperature. The total flux of  $\text{CO}_2$ , constant with respect to the diffusion path  $x$ , is given by the sum of the (variable) fluxes of dissolved  $\text{CO}_2$  and bicarbonate:

$$F_{\text{tot}} = F_{\text{CO}_2} + F_{\text{HCO}_3^-}. \quad (2)$$

The condition of equivalent fluxes of bicarbonate and protons, the condition of zero fluxes of the ions not participating in the transport process, as well as the condition of zero net charge movement, are ensured by the following equations:

$$F_{\text{HCO}_3^-} = F_{\text{H}_2\text{PO}_4^-} = -F_{\text{HPO}_4^{--}}; \quad (3)$$

$$F_{\text{Na}^+} = F_{\text{K}^+} = 0. \quad (4)$$

In Eq. 3, the fluxes of free protons and hydroxyl ions are neglected. Since only  $\text{CO}_2$  fluxes not limited by the  $\text{CO}_2$  hydration velocity shall be considered, all reactions involved may be assumed to be in equilibrium:

$$\frac{[\text{HCO}_3^-] \cdot [\text{H}_2\text{PO}_4^-]}{[\text{CO}_2] \cdot [\text{HPO}_4^{--}]} = \frac{K_{\text{CO}_2}}{K_{\text{phosphate}}} \quad (5)$$

Finally, electroneutrality is taken to be established everywhere in the layer:

$$\sum z_i \cdot c_i = 0. \quad (6)$$

These equations were integrated numerically within the limits  $x = 0$  and  $x = 1$  using Euler's method (29) on a 12-digit Wang calculator (Wang Laboratories Inc., Tewksbury, Mass.). They were solved in a way to obtain a theoretical value of  $F_{\text{tot}}$  for the boundary conditions of the experiment considered.

The following boundary conditions were employed:  $[\text{CO}_2]$  ( $x = 0$ ) and  $[\text{CO}_2]$  ( $x = 1$ ) are those of the experiment, the average total concentration of phosphate in the layer ( $1^{-1} \int_{x=0}^1 [\text{H}_2\text{PO}_4^-] dx + 1^{-1} \int_{x=0}^1 [\text{HPO}_4^{--}] dx$ ) is that of the solution used in the experiment, the average concentration of primary phosphate ( $1^{-1} \int_{x=0}^1 [\text{H}_2\text{PO}_4^-] dx$ ) equals its original concentration in the used solution at  $p\text{CO}_2 = 0$  plus the average bicarbonate concentration in the layer ( $1^{-1} \int_{x=0}^1 [\text{HCO}_3^-] dx$ ), and  $\phi$  ( $x = 0$ ) = 0.

#### *Comparison of Experimental and Theoretical Results*

Using the constants given in Tables I and III the total fluxes of  $\text{CO}_2$  were calculated for the conditions of the experiments represented by Fig. 1: For the 66 mM solution a  $\text{CO}_2$  flux of  $3.0 \text{ nmol cm}^{-2}\text{s}^{-1}$  was obtained, which compares with the measured maximal flux of  $3.2 \text{ nmol cm}^{-2}\text{s}^{-1}$  (Fig. 1 *a*). In the case of the 705 mM solution a  $\text{CO}_2$  flux of  $3.5 \text{ nmol cm}^{-2}\text{s}^{-1}$  is predicted by the model while the measured flux is  $3.4 \text{ nmol cm}^{-2}\text{s}^{-1}$  (Fig. 1 *b*). These good agreements indicate that the model of facilitated  $\text{CO}_2$  diffusion represented in Fig. 4 can quantitatively account for the measured facilitated  $\text{CO}_2$  fluxes. We conclude that facilitated proton transport by phosphate diffusion appears to be a mechanism indeed 10,000 times more effective than free proton diffusion.

#### *Concentration Profiles in the Layer*

Fig. 5 illustrates how a proton flux equivalent to the flux of bicarbonate is achieved by interaction of the concentration gradients of the transporting ions and the gradient of the diffusion potential. It shows calculated concentration profiles of  $\text{CO}_2$ ,  $\text{HCO}_3^-$ ,  $\text{H}_2\text{PO}_4^-$ , and  $\text{HPO}_4^{--}$  in the layer, together with the profile of the electrical potential. The figure refers to an experiment with 66 mM phosphate solution,  $\text{CO}_2$  boundary partial pressures of 57 and 26 torr, and excess carbonic anhydrase (Fig. 1 *a*). The boundary pH values, as calculated from the boundary ion concentrations, are 6.89 and 7.07. All profiles, including that of the electrical potential, show slight deviations from linearity: the gradients of the ions and of the diffusion potential are 25% greater at  $x = 1$  (side of low  $p\text{CO}_2$ ) than at  $x = 0$  (side of high  $p\text{CO}_2$ ), while the gradient of  $\text{CO}_2$  is 45% greater at  $x = 0$  than at  $x = 1$ . The diffusion coefficients used for the calculations in this example were:  $D_{\text{CO}_2} = 15.9$ ,  $D_{\text{HCO}_3^-} = 8.7$ ,  $D_{\text{H}_2\text{PO}_4^-} = 7.0$ ,  $D_{\text{HPO}_4^{--}} = 2.4$ , all in the unit  $10^{-6} \text{ cm}^2\text{s}^{-1}$  (see Appendix). It can be understood from the profiles shown in Fig. 5 how, for instance, equimolar fluxes of  $\text{HPO}_4^{--}$  and  $\text{HCO}_3^-$  are

brought about, even though the diffusion coefficient of  $\text{HPO}_4^{--}$  is only 28% of that of  $\text{HCO}_3^-$ : (a) the concentration difference of  $\text{HPO}_4^{--}$  across the layer is about twice that of  $\text{HCO}_3^-$ , and (b) the electrical potential difference across the layer,  $-1.4$  mV, increases the diffusional flux of  $\text{HPO}_4^{--}$  by 52% and decreases the flux of  $\text{HCO}_3^-$  by 17%.<sup>1</sup> Similarly, the diffusional flux of  $\text{H}_2\text{PO}_4^-$  is reduced by 26% through the diffusion potential. The concentration and potential profiles obtained for the experiment with 705 mM phosphate solution are very much like those of Fig. 5. We conclude that an adequate description of facilitated

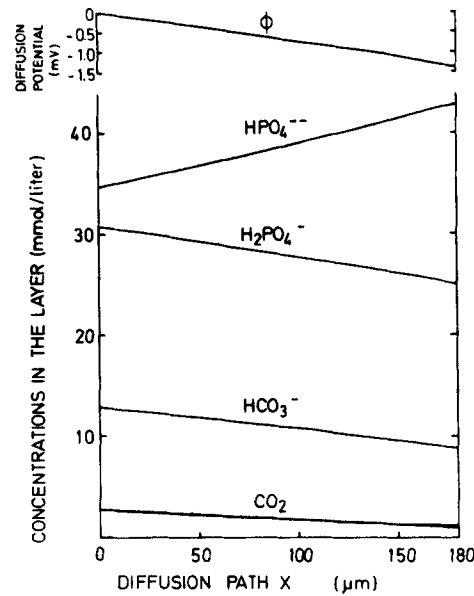


FIGURE 5. Calculated concentration profiles of  $\text{CO}_2$ ,  $\text{HCO}_3^-$ ,  $\text{H}_2\text{PO}_4^-$ , and  $\text{HPO}_4^{--}$  in a  $180\text{-}\mu\text{m}$ -thick Millipore layer, together with the profile of the diffusion potential,  $\phi$ . The figure refers to the experimental conditions of Fig. 1 a: 66 mM phosphate solution, carbonic anhydrase concentration  $\geq 0.2$  g/100 ml,  $\text{CO}_2$  boundary partial pressures 57 and 26 torr, respectively. The boundary pH values (not shown) were calculated to be 6.89 and 7.07.

$\text{CO}_2$  diffusion in phosphate solutions has to take into account the diffusion potentials which in this case are large enough to have a significant effect on the ionic fluxes.

<sup>1</sup> The ratio of the ion flux mediated by the electrical field over the ion flux due to the concentration gradient is

$$\frac{D_i FR^{-1} T^{-1} z_i C_i \cdot d\phi/dx}{D_i dC_i/dx} \approx \frac{z_i \bar{C}_i}{\Delta C_i} \cdot \frac{\Delta\phi}{25.7 \text{ mV}}$$

as may be derived from Eq. 1. Since  $\text{HPO}_4^{--}$  under the present conditions exhibits the highest average concentration in the layer,  $\bar{C}_i$ , as well as charge,  $z_i$ , of all ions involved, the value of  $z_i \bar{C}_i / \Delta C_i$  is greatest for  $\text{HPO}_4^{--}$ . Thus, the flux of this ion is affected most by the electrical potential difference,  $\Delta\phi$ .

*Facilitated CO<sub>2</sub> Diffusion as a Function of pCO<sub>2</sub>*

In Fig. 6 *a* the CO<sub>2</sub> flux across a 180- $\mu$ m-thick layer of 66 mM phosphate solution (pH = 7.30 at pCO<sub>2</sub> = 0) calculated for a constant pCO<sub>2</sub> difference of 10 torr is plotted versus the average pCO<sub>2</sub> in the layer. It can be seen that facilitated diffusion depends strongly on the pCO<sub>2</sub>: For an average pCO<sub>2</sub> of 5.2 torr the total flux of CO<sub>2</sub> is 5.3 times higher than is expected from free diffusion of CO<sub>2</sub> alone. Increasing the average pCO<sub>2</sub> to 100 torr leads to a sharp decrease of the total CO<sub>2</sub> flux to the 1.6-fold of the flux by free diffusion. With further increasing pCO<sub>2</sub> the total CO<sub>2</sub> flux then approaches gradually the flux by free diffusion. The reason for this behavior becomes clear from Fig. 6 *b*, where the calculated concentration differences of H<sub>2</sub>PO<sub>4</sub><sup>-</sup> (i.e. of buffered protons) and of

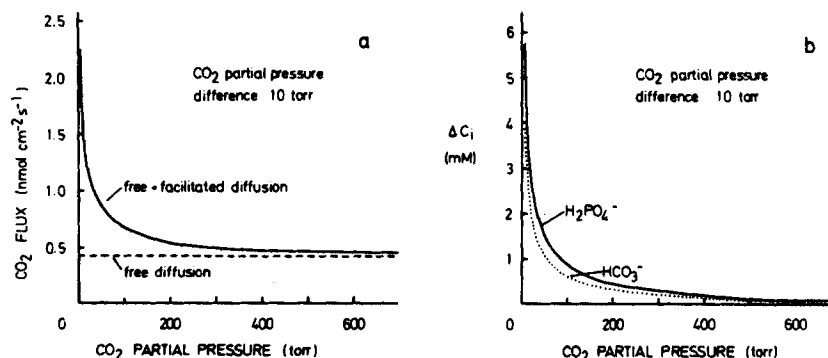


FIGURE 6. (a) Calculated CO<sub>2</sub> fluxes at a constant CO<sub>2</sub> partial pressure difference of 10 torr as a function of the average pCO<sub>2</sub> in the layer. The boundary CO<sub>2</sub> partial pressure at the side of low pCO<sub>2</sub> was varied from 0.2 to 690 torr. Solution: 66 mM phosphate (49 mM Na<sub>2</sub>HPO<sub>4</sub> + 17 mM KH<sub>2</sub>PO<sub>4</sub>, pH 7.3 at pCO<sub>2</sub> = 0). Thickness of the layer 180  $\mu$ m. The solid curve shows the total flux of CO<sub>2</sub>, the dashed curve represents the flux by free diffusion of CO<sub>2</sub> only. (b) Concentration differences,  $\Delta C_i$ , of HCO<sub>3</sub><sup>-</sup> and H<sub>2</sub>PO<sub>4</sub><sup>-</sup> as functions of the average pCO<sub>2</sub> in the layer. The curves are calculated for the conditions of Fig. 6 *a*.

HCO<sub>3</sub><sup>-</sup> across the layer are plotted as a function of the average pCO<sub>2</sub>:  $\Delta[\text{HCO}_3^-]$  as well as  $\Delta[\text{H}_2\text{PO}_4^-]$  decrease with increasing pCO<sub>2</sub> in a fashion quite similar to that of the facilitated CO<sub>2</sub> flux. This phenomenon reflects the hyperbolic shape of CO<sub>2</sub> binding curves in buffer solutions. This shape implies that a given CO<sub>2</sub> partial pressure difference is accompanied by a larger concentration difference of bicarbonate and of buffered protons in a low rather than in a high partial pressure range. A qualitatively similar dependence on the partial pressure range has been demonstrated for facilitated oxygen diffusion in hemoglobin solutions (11).

*Facilitated CO<sub>2</sub> Diffusion as a Function of pH*

In Fig. 7 *a* the flux of CO<sub>2</sub> at constant boundary pCO<sub>2</sub>'s of 50 and 40 torr, respectively, is plotted versus the average pH in the layer. The fluxes are again calculated for a 180- $\mu$ m-thick layer of 66 mM phosphate solution. It can be seen

that facilitated diffusion occurs already at pH 5.8 and increases with pH to reach a maximum (150% of free diffusion) at pH 7.3. With further increasing pH the facilitation of CO<sub>2</sub> diffusion then decreases and reaches a value of 84% at pH 7.9.

It seems striking that facilitated diffusion does not reach its maximum exactly at pH 6.84, the pK value of the phosphate (see Table III) where the solution has its maximal buffer capacity, but about half a pH unit above that. This pattern of pH dependence is due to the CO<sub>2</sub> binding characteristics of the phosphate solution: Whereas above pH 6.84 the buffer capacity of the phosphate solution decreases, the pH difference across the layer markedly increases as shown in

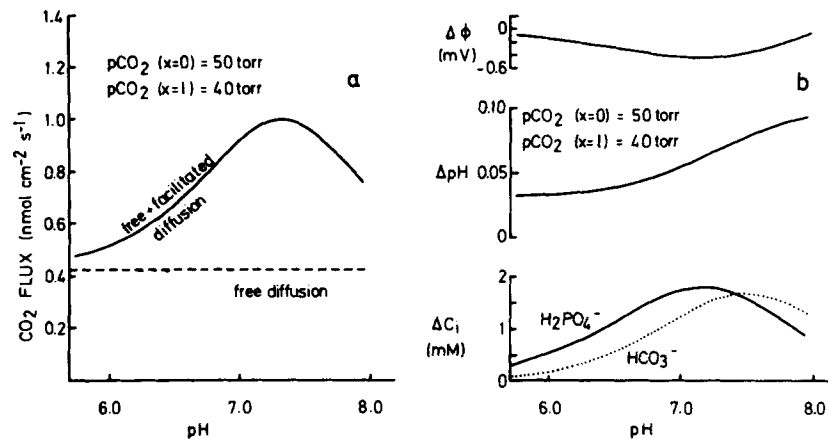


FIGURE 7. (a) Calculated CO<sub>2</sub> fluxes as a function of the average pH value in the layer. The boundary CO<sub>2</sub> partial pressures are constant with 50 and 40 torr, respectively. The solution is 66 mM phosphate with varying contents of base. Thickness of the layer is 180  $\mu\text{m}$ . The solid curve represents the total flux of CO<sub>2</sub>, the dashed curve the flux by free diffusion only. (b) Concentration differences across the layer,  $\Delta C_i$ , for HCO<sub>3</sub><sup>-</sup> and H<sub>2</sub>PO<sub>4</sub><sup>-</sup>, pH difference,  $\Delta\text{pH}$ , and electrical potential difference,  $\Delta\phi$ , as a function of the average pH in the layer. All curves are calculated for the conditions of Fig. 7 a. The difference of the electrical potential across the layer varies between -0.09 and -0.42 mV and has only a minor influence on the fluxes of HCO<sub>3</sub><sup>-</sup> and H<sub>2</sub>PO<sub>4</sub><sup>-</sup> in the pH and pCO<sub>2</sub> range occurring in the figure.

Fig. 7 b. The sum of these two effects leads to an increase of the concentration differences of HCO<sub>3</sub><sup>-</sup> and of the proton-carrying H<sub>2</sub>PO<sub>4</sub><sup>-</sup> beyond pH 6.84. For the given boundary partial pressures of 50 and 40 torr the concentration differences reach maxima at pH 7.5 for HCO<sub>3</sub><sup>-</sup> and pH 7.2 for H<sub>2</sub>PO<sub>4</sub><sup>-</sup>, resulting in a maximum of facilitated diffusion at pH 7.3. It may be noted that the mechanism of facilitated CO<sub>2</sub> diffusion described by Ward and Robb (19), CO<sub>3</sub><sup>2-</sup>-facilitated proton transport with HCO<sub>3</sub><sup>-</sup> diffusion, contributes less than 2% to the flux of CO<sub>2</sub> in the entire pH range considered in Fig. 7, and thus can be neglected.

Fig. 7 a allows us to estimate the facilitation of CO<sub>2</sub> transfer in a 66 mM phosphate solution under conditions of pCO<sub>2</sub> (40–50 torr) and pH (7.0) as they may occur inside cells. We find a 2.2-fold increase as compared to free diffusion.

## CONCLUSION

A phosphate solution, as used in these experiments, can be considered as a model of the cell interior with respect to proton transport properties. Muscle, for instance, has a total intracellular phosphate concentration of 140 mM (2), and although most of it is organic phosphate, whose diffusion coefficient may be 1.5–2 times lower than that of inorganic phosphate, its capacity to transport protons may be of the same order as that of the 66 mM solution used here. In addition, other mobile buffers encountered in cytoplasm, such as proteins and weak acids, will act as proton carriers in a similar way as phosphate (1, 3, 23).

We may conclude that a powerful mechanism of proton transport acts inside the cell to keep pH gradients small and ensure adequate proton fluxes. Almost all protons dissociated from fixed acids will be transported intracellularly via this mechanism. Cells, which not only contain buffers but also carbonic anhydrase, as erythrocytes and cells in the kidney or gastric mucosa do, should, besides the facilitation of fixed acid transfer, exhibit an improved intracellular CO<sub>2</sub> transfer based on the same proton transport mechanism. Facilitated diffusion of CO<sub>2</sub> has indeed been shown to occur in red cells (30, 31) and very recently even in skeletal muscle cells (32) in which carbonic anhydrase is believed to be low. In cells with high carbonic anhydrase concentrations more than half of the CO<sub>2</sub> transport may occur by facilitated diffusion.

## APPENDIX

To calculate the CO<sub>2</sub> fluxes predicted by the described model of facilitated CO<sub>2</sub> diffusion, knowledge of the dissociation constants of CO<sub>2</sub> and phosphate, and of the diffusion coefficients of HCO<sub>3</sub><sup>-</sup>, H<sub>2</sub>PO<sub>4</sub><sup>-</sup> and HPO<sub>4</sub><sup>2-</sup> valid for the pertinent experimental conditions was necessary (see Eqs. 1 and 5). These constants were derived from the CO<sub>2</sub> binding studies described under Methods and are compiled in Table III. They were calculated as follows.

The dissociation constant of CO<sub>2</sub>,  $K_{CO_2}$ , is defined by the following equation:

$$K_{CO_2} = \frac{a_{H^+} [HCO_3^-]}{[CO_2]}, \quad (7)$$

TABLE III  
CONSTANTS USED FOR THE QUANTITATIVE ANALYSIS OF THE MODEL

Conditions	$pK_{CO_2}$	$pK_{phosphate}$	$\frac{\gamma_{HCO_3^-}}{\gamma_{H_2PO_4^-}} =$	$\lambda_{HPO_4^{2-}}$	$D_{HCO_3^-}$ $cm^2 \cdot s^{-1}$	$D_{H_2PO_4^-}$ $cm^2 \cdot s^{-1}$	$D_{HPO_4^{2-}}$ $cm^2 \cdot s^{-1}$
Infinitely diluted solution	6.35	7.20	—	—	$11.7 \cdot 10^{-6}$	$9.5 \cdot 10^{-6}$	$7.5 \cdot 10^{-6}$
49 mM Na <sub>2</sub> HPO <sub>4</sub> + 17 mM KH <sub>2</sub> PO <sub>4</sub> (pCO <sub>2</sub> 15–70 torr)	6.22 (±0.01)	6.84 (±0.01)	0.74	0.32	$8.7 \cdot 10^{-6}$	$7.0 \cdot 10^{-6}$	$2.4 \cdot 10^{-6}$
666 mM Na <sub>2</sub> HPO <sub>4</sub> + 39 mM KH <sub>2</sub> PO <sub>4</sub> (pCO <sub>2</sub> 15–70 torr)	5.93 (±0.01)	6.46 (±0.01)	0.38	0.069	$4.4 \cdot 10^{-6}$	$3.6 \cdot 10^{-6}$	$0.52 \cdot 10^{-6}$

Dissociation constants of CO<sub>2</sub> and phosphate,  $pK_{CO_2}$  and  $pK_{phosphate}$  (with standard errors), and activity and diffusion coefficients,  $\gamma$  and  $D$ , of HCO<sub>3</sub><sup>-</sup>, H<sub>2</sub>PO<sub>4</sub><sup>-</sup>, and HPO<sub>4</sub><sup>2-</sup> under different conditions of ionic strength. Temperature 25°C. The  $pK_{CO_2}$  values are calculated using the CO<sub>2</sub> solubilities given in the legend of Table I. All data at infinite dilution are taken from Landolt and Börnstein (33). Activity and diffusion coefficients in the phosphate solutions are calculated using the experimentally determined dissociation constants.

where  $a_{H^+}$  is the  $H^+$  activity and assumed to be given by the pH measured with the glass electrode,  $[HCO_3^-]$  and  $[CO_2]$  are the concentrations of bicarbonate and dissolved  $CO_2$ , respectively. The three parameters on the right-hand side of Eq. 7 were determined at 5  $CO_2$  partial pressures between 15 and 70 torr, which approximately covers the  $pCO_2$  range occurring inside the diffusion layers (see Table I). For each  $pCO_2$  a value of  $K_{CO_2}$  was calculated. Taking the average of all values of  $K_{CO_2}$  should yield a value valid for the average ionic strength prevailing in the layers during the diffusion experiments.  $K_{CO_2}$  thus obtained is listed in Table III for the 66 and 705 mM phosphate solution. The dissociation constant of phosphate,  $K_{phosphate}$ , is defined by:

$$K_{phosphate} = \frac{a_{H^+} [HPO_4^{--}]}{[H_2PO_4^-]}, \quad (8)$$

where  $[HPO_4^{--}]$  and  $[H_2PO_4^-]$  are the concentrations of di- and monovalent phosphate, respectively. Making use of the fact that an increase in the concentration of bicarbonate due to a rise in  $pCO_2$  is accompanied by an equal increase in the concentration of  $H_2PO_4^-$  ( $HPO_4^{--} + CO_2 + H_2O \rightleftharpoons H_2PO_4^- + HCO_3^-$ ), we may write:

$$[H_2PO_4^-] = [H_2PO_4^-]_{(pCO_2=0)} + [HCO_3^-], \quad (9)$$

and

$$[HPO_4^{--}] = [HPO_4^{--}]_{(pCO_2=0)} - [HCO_3^-]. \quad (10)$$

where the index ( $pCO_2 = 0$ ) indicates the concentrations of the respective phosphate ions when  $pCO_2 = 0$ . Thus, knowing the bicarbonate concentrations and the original composition of the  $CO_2$ -free phosphate solutions the average values of  $K_{phosphate}$  for the  $pCO_2$  range of interest could be calculated.

The diffusion coefficients of ions may be estimated as the product of their diffusion coefficients at infinite dilution and their activity coefficients in the pertinent ionic milieu. Diffusion coefficients of ions at infinite dilution are readily calculated from their equivalent conductivities at infinite dilution on which extensive data are available in the literature (33). The activity coefficients of the ions involved were obtained from the values of  $K_{CO_2}$  and  $K_{phosphate}$  shown in Table III, thus ensuring that they are valid for the conditions of the present diffusion experiments. The  $CO_2$  dissociation constant at infinite dilution is given by:

$$K_{CO_2(0)} = \frac{a_{H^+} \cdot [HCO_3^-] \cdot \gamma_{HCO_3^-}}{[CO_2]}, \quad (11)$$

where  $\gamma_{HCO_3^-}$  is the activity coefficient of bicarbonate.

Accordingly,  $\gamma_{HCO_3^-}$  can be calculated from:

$$\gamma_{HCO_3^-} = \frac{K_{CO_2(0)}}{K_{CO_2}}, \quad (12)$$

where  $K_{CO_2(0)}$  may be taken from the literature (33). Assuming that the activity coefficients of the two monovalent ions involved are identical

$$\gamma_{H_2PO_4^-} = \gamma_{HCO_3^-}, \quad (13)$$

we arrive, by a similar consideration, at an expression for the activity coefficient of the divalent phosphate ion:

$$\gamma_{HPO_4^{--}} = \frac{K_{phosphate(0)}}{K_{phosphate}} \cdot \gamma_{HCO_3^-}, \quad (14)$$

where  $K_{\text{phosphate}}^{(0)}$  is the dissociation constant of phosphate at infinite dilution. The activity coefficients of the three ions obtained in this way are listed in Table III together with their diffusion coefficients.

The authors are grateful to Dr. C. Bauer, Regensburg, for directing their attention to cellulose phosphate P11.

Received for publication 14 November 1975.

#### REFERENCES

1. GROS, G., and W. MOLL. 1974. Facilitated diffusion of  $\text{CO}_2$  across albumin solutions. *J. Gen. Physiol.* **64**:356-371.
2. PITTS, R. F. 1963. Physiology of the Kidney and Body Fluids. Year Book Medical Publishers, Inc., Chicago. 28.
3. GROS, G., and W. MOLL. 1972. The facilitated diffusion of  $\text{CO}_2$  in hemoglobin solutions and phosphate solutions. In *Oxygen Affinity of Hemoglobin and Red Cell Acid Base Status*. M. Rørth and P. Astrup, editors. Munksgaard, Copenhagen. 483-492.
4. ENGASSER, J. M., and C. HORVATH. 1974. Buffer facilitated proton transport. pH profile of bound enzymes. *Biochim. Biophys. Acta.* **358**:178-192.
5. FATT, I., and R. C. LA FORCE. 1961. Theory of oxygen transport through hemoglobin solutions. *Science (Wash. D.C.)*. **133**:1919-1921.
6. COLLINS, R. E. 1961. Transport of gases through hemoglobin solution. *Bull. Math. Biophys.* **28**:223-232.
7. WITTENBERG, J. B. 1966. The molecular mechanism of hemoglobin-facilitated oxygen diffusion. *J. Biol. Chem.* **241**:104-114.
8. MOLL, W. 1966. The diffusion coefficient of haemoglobin. *Respir. Physiol.* **1**:357-365.
9. KUTCHAI, H., and N. C. STAUB. 1969. Steady-state, hemoglobin-facilitated  $\text{O}_2$  transport in human erythrocytes. *J. Gen. Physiol.* **53**:576-589.
10. MOLL, W. 1969. Measurements of facilitated diffusion of oxygen in red blood cells at  $37^\circ\text{C}$ . *Pfluegers Arch. Eur. J. Physiol.* **305**:269-278.
11. SCHOLANDER, P. F. 1960. Oxygen transport through hemoglobin solutions. *Science (Wash. D.C.)*. **131**:585-590.
12. GROS, G., and W. MOLL. 1971. The diffusion of carbon dioxide in erythrocytes and hemoglobin solutions. *Pfluegers Arch. Eur. J. Physiol.* **324**:249-266.
13. BARTELS, H., E. BÜCHERL, C. W. HERTZ, G. RODEWALD, and M. SCHWAB. 1959. Lungenfunktionsprüfungen. Springer-Verlag, Berlin.
14. Handbook of Chemistry and Physics, 36<sup>th</sup> edition. 1954-1955. C. D. Hodgman, editor. Chemical Rubber Publishing Co., Ohio.
15. VAN SLYKE, D. D., J. SENDROY, A. B. HASTINGS, and J. M. NEILL. 1928. Studies of gas and electrolyte equilibria in blood. X. The solubility of carbon dioxide at  $38^\circ$  in water, salt solution, serum, and blood cells. *J. Biol. Chem.* **78**:765-799.
16. RATCLIFF, G. A., and J. G. HOLDCROFT. 1963. Diffusivities of gases in aqueous electrolyte solutions. *Trans. Inst. Chem. Eng.* **41**:315-319.
17. ROUGHTON, F. J. W., and V. H. BOOTH. 1938. The catalytic effect of buffers on the reaction  $\text{CO}_2 + \text{H}_2\text{O} \rightleftharpoons \text{H}_2\text{CO}_3$ . *Biochem. J.* **32**:2049-2069.
18. LONGMUIR, I. S., R. E. FORSTER, and C. Y. WOO. 1966. Diffusion of carbon dioxide through thin layers of solution. *Nature (Lond.)*. **209**:393-394.
19. WARD, W. J., and W. L. ROBB. 1967. Carbon dioxide-oxygen separation: Facilitated

- transport of carbon dioxide across a liquid film. *Science (Wash. D.C.)*. **156**:1481-1484.
20. SUCHDEO, S. R., and J. S. SCHULTZ. 1974. Mass transfer of CO<sub>2</sub> across membranes: facilitation in the presence of bicarbonate ion and the enzyme carbonic anhydrase. *Biochim. Biophys. Acta*. **352**:412-440.
  21. ENNS, T. 1967. Facilitation by carbonic anhydrase of carbon dioxide transport. *Science (Wash. D.C.)*. **155**:44-47.
  22. DONALDSON, T. L., and J. A. QUINN. Kinetic constants determined from membrane transport measurements: carbonic anhydrase activity at high concentrations. *Proc. Natl. Acad. Sci. U.S.A.* **71**:4995-4999.
  23. GROS, G. 1969. Die freie und erleichterte Diffusion von Kohlendioxid in Erythrocyten und Hämoglobinlösungen. M.D. Thesis. Universität Tübingen, Tübingen.
  24. KORTÜM, G. 1972. Lehrbuch der Elektrochemie. Verlag Chemie, Weinheim/Bergstr. 5th edition. 263.
  25. EINSTEIN, A. 1906. Eine neue Bestimmung der Moleküldimensionen. *Ann. Physik*. **19**:289-306.
  26. HIMMELBLAU, D. M. 1964. Diffusion of dissolved gases in liquids. *Chem. Rev.* **64**:527-549.
  27. SCHANTZ, E. J., and M. A. LAUFFER. 1962. Diffusion measurements in agar gel. *Biochemistry*. **1**:658-663.
  28. MELDON, J. H., K. A. SMITH, and C. K. COLTON. The effect of weak acids upon the transport of carbon dioxide in alkaline solutions. *Chem. Eng. Sci.* In press.
  29. ZURMÜHL, R. 1965. Praktische Mathematik. Springer-Verlag, Berlin. 5th edition. 388.
  30. ENNS, T., G. B. SHAM, and S. ANDERSON. 1966. Carbonic anhydrase diffusion of CO<sub>2</sub> in whole blood. *Physiologist*. **9**:176.
  31. MOLL, W., and G. GROS. 1966. Untersuchungen über den Gasaustausch der Erythrocyten. *Pfluegers Archiv. Gesamte Physiol. Menschen Tiere*. **291**:54.
  32. SCHEID, P., and T. KAWASHIRO. Measurement of diffusivity of CO<sub>2</sub> in respiring muscle at various CO<sub>2</sub> levels: evidence for facilitated diffusion. *Pfluegers Arch. Eur. J. Physiol.* In press.
  33. LANDOLT, H., and R. BÖRNSTEIN. 1960. Zahlenwerte und Funktionen, Vol. II (7). K. H. Hellwege, A. M. Hellwege, K. Schäfer, and E. Lax, editors. Springer-Verlag, Berlin. 259, 843-844.